Density Functional Theory Study on Metal Bis(trifluoromethylsulfonyl)imides: Electronic Structures, Energies, Catalysis, and Predictions

X. Yong Li and Jin Nie*

Department of Chemistry, Huazhong University of Science and Technology, Wuhan 430074, People's Republic of China

Received: November 7, 2002; In Final Form: March 17, 2003

Theoretical studies on metal bis(trifluoromethylsulfonyl)imides, $M(TFSI)_2$ (M = Mg, Ca, Ba, Zn, and Cu) are carried out using density functional theory (DFT) method and B3LYP/lanl2dz theory level for the first time. Quadradentate structures involving four oxygen atoms of four $-SO_2-$ groups are preferred. Based on these conformations, binding energies and frontier molecular orbital (FMO) energies have been compared, correlated with experimental results, to evaluate the Lewis acidity and catalytic activity of these metal complexes. Wave function analyses have been performed by natural bond orbital (NBO) method to further investigate the cation−anion interactions. $M(TFSI)_2$−acrolein complexes are also calculated at the same level to obtain a better understanding of the interactions between Lewis acid and dienophile. Several important trends are revealed and give an insight into the molecular structures and Lewis acidity of $M(TFSI)_2$, as well as the weakly coordinating property of $TFSI^-$ anion. Explanations for the outstanding catalytic property of $Cu(TFSI)_2$ are put forward. Predictions upon a novel Lewis acid are also provided.

Introduction

In recent years, "weakly coordinating" anions[1−3] have caused great interest among chemists. As an outstanding weakly coordinating anion, the TFSI ($N(SO_2CF_3)_2$) imide anion[4] and its metal complexes have been extensively investigated in the development of highly effective Lewis acid catalysts[5−9] and novel electrolytes.[10−12]

Generally, the focus on development of the novel Lewis acid catalyst has been on seeking a proper anion for coordination with various kinds of metal cations to obtain desired species with appropriate Lewis acidity, as well as catalytic property. This usually is a time-consuming project and sometimes even an aimless one. To save both time and resources and to make the exploration more definite, a theoretical approach is undoubtedly necessary and is attracting attentions of more and more chemists.

To the best of our knowledge, theoretical research of metal bis(trifluoromethylsulfonyl)imides through quantum chemical calculations is very limited besides several reports about LiTFSI, TFSI anion, and HTSFI acid.[13−17] All of these works only focused on the conformation and electrochemistry of the species. No computational study on the structure and catalytic property of $M(TFSI)_2$ (M = Mg, Ca, Ba, Zn, and Cu) was seen. Experimental data on the structures were also limited,[18,19] which makes us remain unclear about the microstructures of metal bis(trifluoromethylsulfonyl)imides. While, as we know, the anion−cation interaction within Lewis acid plays an important role to its Lewis acidity, as well as catalytic property. So, a thorough computational investigation on the electronic structures, energies, and orbitals of $M(TFSI)_2$ would be quite necessary and helpful to better our understanding to a quantum level.

Ab initio quantum chemistry method up to 6-31+G* level is often employed in the theoretical study on LiTFSI. This method is unsuitable and impracticable for our molecule system because (1) such metal complexes are relatively large in size and contain heavy metal atoms and (2) electron correlations have considerable effects on binding energies but they are usually unaccounted for a traditional Hatree-Fock calculation. So density functional theory (DFT) B3LYP method[20,21] in conjugation with standard lanl2dz basis set[22] is chosen for our calculation. This method has been very common because it accounts better for electron correlation energies and greatly reduces the calculation expenses with reliable description of both geometries and energetics[23,24] for systems containing heavy atoms.

In this paper, we report the computational study on $M(TFSI)_2$ (M = Mg, Ca, Ba, Zn, and Cu) complexes for the first time. Several trends are revealed and reasonable predictions are then made upon the novel Lewis acid synthesizing in our lab.

Calculation Method

Preoptimization was performed using semiempirical PM3-(PM3/D) method[25] to locate the preferred positions for metal ion coordination, as well as to provide staring geometries for higher level calculations. $Ba(TFSI)_2$ and the new synthesized compound were preoptimized by MMFF94 molecular mechanics force field[26] calculation because of the lack of parameters for heavy atoms Ba and La in semiempirical method. The metal ion's starting position was initially chosen to be adjacent to the negative parts (nitrogen atoms and oxygen atoms in SO_2 groups) of the anion.

Subsequently, all of the metal complexes were treated with DFT method at B3LYP/lanl2dz level for full geometry optimization. Nature population analysis (NPA) and natural bond orbital (NBO) analysis were performed at the same level using NBO program 3.1[27] to obtain quantitative analysis of cation−anion interactions between NBOs of Lewis acids. Quantitative study of interactions between Lewis acids and dienophile were also obtained through NBO analysis and frontier molecular orbital (FMO) energetic calculations.

* To whom correspondence should be addressed. E-mail: niejin@mail.hust.edu.cn.

10.1021/jp022383o CCC: $25.00
Published on Web 07/10/2003

TABLE 1: Main Geometry Parameters of $M(TFSI)_x$ and TFSI Anion

	$Cu(TFSI)_2$	$Zn(TFSI)_2$	$Mg(TFSI)_2$	$Ca(TFSI)_2$	$Ba(TFSI)_2$	LiTFSI	$TFSI^-$
M−N1	3.834	3.904	3.816	4.181	4.525	3.640	
M−N2	3.834	3.904	3.816	4.181	4.525		
M−O1	1.960	1.996	1.967	2.559	2.907	1.832	
M−O2	1.955	1.996	1.972	2.350	2.665	1.832	
M−O3	1.960	1.996	1.972	2.556	2.907		
M−O4	1.955	1.996	1.967	2.355	2.663		
M−O5				2.616	2.935		
M−O7				2.609	2.935		
N1−S1	1.808	1.818	1.810	1.792	1.794	1.810	1.808
N1−S2	1.822	1.818	1.830	1.846	1.835	1.810	1.808
N2−S3	1.822	1.818	1.830	1.791	1.794		
N2−S4	1.808	1.818	1.810	1.847	1.835		
S1−O1	1.685	1.672	1.660	1.656	1.649	1.650	1.628
S2−O2	1.685	1.672	1.663	1.645	1.645	1.650	1.628
S3−O3	1.685	1.672	1.663	1.656	1.6649		
S4−O4	1.685	1.672	1.660	1.645	1.645		
S1−O5(3)	1.607	1.608	1.607	1.654	1.648	1.610	1.628
S2−O6(4)	1.610	1.608	1.611	1.606	1.608	1.610	1.628
S3−O7	1.610	1.608	1.611	1.655	1.648		
S4−O8	1.607	1.608	1.607	1.606	1.608		
S1−N1−S2	110.9	113.6	113.4	107.7	109.1	115.3	117.6
S3−N2−S4	110.9	113.6	113.4	107.5	109.1		

Single-point energy calculations at higher level basis set (B3LYP/6-31G*//B3LYP/lanl2dz) were also performed to obtain more accurate binding energies, which were defined as $E_{bind} = E_{metalcomplex} - (E_{cation-free} + E_{anion-free})$.

Lewis acidity and catalytic ability of these metal complexes were quantitatively evaluated according to FMO energies, effective ionic charges, and NBO interaction energies correlated with experimental results.[5] Theoretical comparisons between $Zn(TFSI)_2$, $Zn(Tf)_2$, and $ZnCl_2$ were also made.

The PM3 and MMFF94 calculation were performed using PC Spartan Pro program.[28] All of the DFT calculations were performed using the Gaussian 98 program package.[29]

Results and Discussion

Geometries. As mentioned in the Introduction, the LiTFSI ion pair has been widely studied by R. Arnaud et al.[14] using ab initio Hartree−Fock method up to 6-31+G* level. Their work shows that the bidentate structures are the most stable. And the linkage in which Li^+ was bounded with an oxygen atom of each SO_2 group in LiTFSI leads to the largest binding energy, as well as the most stable conformation, while no significant interaction between cation and the nitrogen atom of the imide anion was observed. Our calculations agree well with these results; the quadradentate structures in which the metal cations coordinate with four oxygen atoms of the four SO_2 groups hold the lowest total energies. This type of coordination is generally 15−23 kcal/mol more stabilizing than the coordination involving two N atoms. So, only the optimized geometrical parameters of the quadradentate salts are given in Table 1. For comparison, geometrical parameters of the equilibrium structures of free TFSI anion are also included. The obtained energy-minimum structures are depicted in Figure 1.

As depicted in Figure 1, the metal cations prefer to bind with the oxygen atoms in SO_2 groups, while they are far from the nitrogen atoms that are negative centers of the imide anions. The M−N distances (ranging from 3.448 to 4.525 Å) are all much longer than the sum of ionic or covalent radii[30] of the cations and N atom, which indicates no interactions between them. This is in good agreement with the weakly coordinating property of the TFSI anion and further proves that this anion behaves just like an oxyacid anion in this respect.[18] The $Cu(TFSI)_2$ clearly has a planar square coordinating structure (O1−O2−O4−O3 dihedral angle is 2.25°), while other divalent metal complexes have a tetrahedron one. Furthermore, we find that with the increase of cation radius,[30] in the order $Cu^{2+} < Mg^{2+} < Zn^{2+} < Ca^{2+} < Ba^{2+}$, the main M−O bond length also increases from 1.955 Å (Cu−O) to 2.665 Å (Ba−O). As a result, the M−O bond length gradually becomes larger than the sum of ionic radii of the cations and O atom. This clearly suggests the decreasing interactions between cations and O atoms.

One may note that for $Ca(TFSI)_2$ and $Ba(TFSI)_2$, there are two more oxygen atoms (O5 and O7) contacting the cation center at relatively shorter distance. This is perhaps due to the large size of the cations ($r_{Ca^{2+}} = 1.05$ Å, $r_{Ba^{2+}} = 1.38$ Å), which permits them to contact more O atoms. Influence of the extra two metal−oxygen interactions will be discussed later in this paper.

Compared with free TFSI anion, structural changes of the $TFSI^-$ moiety in the divalent salts are as follows: (1) As expected, the cation-unbounded S−O distances are generally shortened by ca. 0.02 Å, whereas the cation-bounded S−O distances are lengthened by the different extent. The biggest increase in the S−O distance was found for $Cu(TFSI)_2$ by 0.057 Å. This is comparable with the ab initio calculation of Arnaud et al. on LiTFSI,[14] in which the Li-unbounded S−O bonds contract by 0.03 Å with the lengthening of Li-bounded S−O bonds by 0.018 Å. (2) For each SO_2 group in copper and alkaline earth metal complexes, one of the two S−N bonds is lengthened by 0.014−0.039 Å, while all of the S−N bond lengths increase by about 0.01 Å in Zn^{2+} complexes. The result of Arnaud et al. also indicated the increase of S−N bonds by 0.02 Å. (3) Finally, the S−N−S angles decrease by 4−10° indicating that a distortion occurs when TFSI anion coordinates with these metal cations. A more obvious distortion up to 19° for S−N−S angle can be observed in the study by Arnaud et al.

All of the structural changes mentioned above agree well with the results of Arnaud et al.[14] for lithium triflate and LiTFSI, as well as with the experimental data about $Mg(TFSI)_2 \cdot 8H_2O$.[18] This demonstrates the reliability of B3LYP/lanl2dz method on geometry characterization.

One point must be mentioned that, in an early experimental study on $M(TFSI)_2PEO_n$ (M = Mg, Ca, Sr, and Ba), Bakker et al.[31] suggested a possible cation coordination for $Ca(TFSI)_2$ and

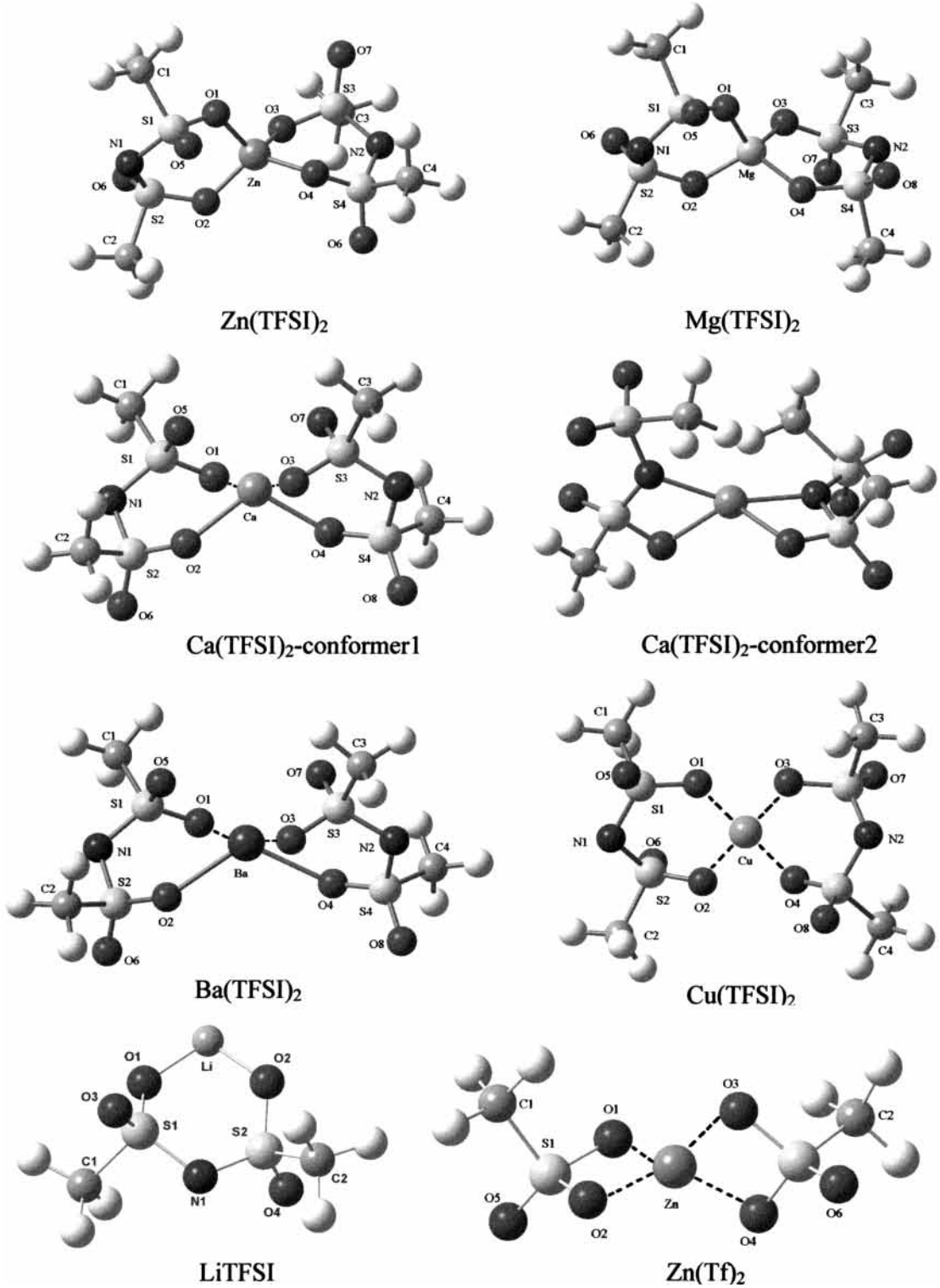

Figure 1. Atomic numbering and equilibrium geometries of $M(TFSI)_x$ (unlabled atoms are F atoms).

$Ba(TFSI)_2$ in which the cation coordinates with the nitrogen atom and an O atom of each anion. This is also depicted in Figure 1 as $Ca(TFSI)_2$-conformer2. But that was obtained according to the behavior at solid state, while our calculation is based on gas phase. Moreover, energetic result shows that the total energy of $Ca(TFSI)_2$-conformer1 (−2138.016 79 au, B3LYP/lanl2dz) is fairly lower (22 kcal/mol) than that of $Ca(TFSI)_2$-conformer2 (−2137.981 95 au B3LYP/lanl2dz), indicating that the former should be the most stable one. Thus, all of the discussions related to $Ca(TFSI)_2$ and $Ba(TFSI)_2$ are based on the four oxygen atoms coordination conformations.

Charges. Mulliken atomic charges and natural charge population (NPA) of $M(TFSI)_2$ and the free TFSI anion are listed in Table 2 to analyze the redistribution of electronic charge in the anion perturbed by the metal cations.

The most striking feature observed is that oxygen atoms directly bounded with metal cations have greater negative charge than that in the free anion (increase by 0.124−0.248 e for NPA), while the metal-unbounded O atoms show less charge compared with the free anion (decrease by 0.080−0.063 electron for NPA). An interesting trend can be easily disclosed for these metal complexes. There are increasing positive charges on cations from

TABLE 2: Mulliken and NPA (in Parentheses) Atomic Charges of $M(TFSI)_x$ and TFSI

	$Cu(TFSI)_2$	$Zn(TFSI)_2$	$Mg(TFSI)_2$	$Ca(TFSI)_2$	$Ba(TFSI)_2$	LiTFSI	$TFSI^-$
M	0.908	1.293	1.438	1.625	1.792	0.743	
	(1.406)	(1.757)	(1.816)	(1.893)	(1.949)	(0.949)	
N1	−0.499	−0.504	−0.505	−0.509	−0.522	−0.520	−0.604
	(−0.902)	(−0.913)	(−0.905)	(−0.901)	(−0.926)	(−0.928)	(−1.007)
N2	−0.499	−0.504	−0.505	−0.509	−0.522		
	(−0.900)	(−0.913)	(−0.899)	(−0.896)	(−0.888)		
O1	−0.612	−0.695	−0.745	−0.614	−0.626	−0.683	−0.557
	(−0.951)	(−1.028)	(−1.058)	(−0.910)	(−0.905)	(−1.001)	(−0.810)
O2	−0.585	−0.695	−0.719	−0.747	−0.753	−0.681	−0.557
	(−0.925)	(−1.028)	(−1.035)	(−1.019)	(−1.013)	(−1.002)	(−0.810)
O3	−0.585	−0.695	−0.719	−0.614	−0.626	−0.477	−0.557
	(−0.926)	(−1.028)	(−1.034)	(−0.910)	(−0.905)	(−0.749)	(−0.810)
O4	−0.612	−0.695	−0.745	−0.747	−0.753	−0.477	−0.557
	(−0.947)	(−1.0281)	(−1.051)	(−1.017)	(−1.003)	(−0.752)	(−0.810)
O5	−0.454	−0.4544	−0.461	−0.5972	−0.6173		
	(−0.721)	(−0.728)	(−0.724)	(−0.894)	(−0.908)		
O6	−0.454	−0.454	−0.464	−0.463	−0.474		
	(−0.728)	(−0.728)	(−0.729)	(−0.727)	(−0.747)		
O7	−0.454	−0.454	−0.464	−0.598	−0.617		
	(−0.729)	(−0.728)	(−0.734)	(−0.896)	(−0.888)		
O8	−0.454	−0.454	−0.461	−0.463	−0.474		
	(−0.722)	(−0.728)	(−0.723)	(−0.729)	(−0.732)		
Z/*r*	1.262	1.558	1.917	1.547	1.299	1.061	
	(1.953)	(2.117)	(2.421)	(1.803)	(1.412)	(1.356)	

TABLE 3: Binding Energies of Various Metal Complexes at B3LYP/lanl2dz and B3LYP/6-31G*//B3LYP/lanl2dz (Bold) Levels[a]

	$Cu(TFSI)_2$	$Zn(TFSI)_2$	$Mg(TFSI)_2$	$Ca(TFSI)_2$	$Ba(TFSI)_2$ [c]	LiTFSI	$Zn(Tf)_2$	$ZnCl_2$
E_{bind} [b]	578.6	536.8	509.3	417.9	359.9	48.4	536.8	604.1
	503.7	**489.7**	**446.5**	**351.4**		**109.7**	**530.5**	**624.9**

[a] Total energies of anions and metal cations are calculated, respectively, at the two levels. [b] In units of kcal/mol. [c] The basis set for Ba is out of range of 6-31G*, so the calculation at B3LYP/6-31G* level cannot be performed for $Ba(TFSI)_2$.

Cu atom to Ba atom. This possibly indicates the degreasing electron transfer from TFSI anion to metal cations. According to the study of Reed et al.,[32] a change in population of 0.001 e corresponds to the change of 0.001 hartree or 0.627 kcal/mol in energy stabilization. Then the largest electron transfer occurring in $Cu(TFSI)_2$ by 0.594 e (NPA charge) corresponds to the largest charge-transfer interaction (E_{CT}) of 372.4 kcal/mol. This kind of charge-transfer interaction (E_{CT}) would be useful to study anion−cation binding interactions.

Energetics. The metal cation−$TFSI^-$ binding energies are summarized in Table 3. To evaluate the influence of different anions on binding interactions, energetic results of zinc triflate and zinc dichloride are also listed in the table. Several important trends concerning binding energies would be pointed out.

First, the calculated order of binding energies from B3LYP/lanl2dz calculation is as follows: $ZnCl_2$ > $Cu(TFSI)_2$ > $Zn(TFSI)_2$ > $Zn(Tf)_2$ > $Mg(TFSI)_2$ > $Ca(TFSI)_2$ > $Ba(TFSI)_2$ > LiTFSI. This is in good agreement with general chemistry knowledge. But one may note that there is a deviation; the TFSI anion is widely known to be a weaker coordinating anion than the Tf^- anion. Therefore, the order of their zinc salts should be reversed. A larger 6-31G* basis set is employed to obtain a more accurate description of energies. The calculated series then becomes $ZnCl_2$ > $Zn(Tf)_2$ > $Cu(TFSI)_2$ > $Zn(TFSI)_2$ > $Mg(TFSI)_2$ > $Ca(TFSI)_2$ > $Ba(TFSI)_2$ > LiTFSI. This clearly gives better agreement and demonstrates the weak coordinating property of TFSI anion. In a very recent DFT study by Rulíšek et al. on the complexation energies of transition metal cations with amino acids[33] and proteins[34] at higher level (B3LYP/6−31 ++G(2df,2pd)), Cu^{2+} complexes always render larger binding energies than Zn^{2+} complexes. As to group 1 and group 2 metal complexes, the same trend of binding energies was also reported in Magnusson's previous theoretical research on metal cation−water adducts.[35] Both of their results strongly proved the reliability and accuracy of our calculation method on energy characterization.

To describe the anion−cation interactions in more detail, natural bond orbital (NBO) analysis at B3LYP/lanl2dz level is carried out to further our understanding of orbital interactions and charge delocalizations. Of particular interests are the interactions between O (bounded with metal cation) lone pairs and antibonding orbitals of metal cation lone pairs. The magnitudes of the interactions are shown in Table 4. Because of the reason discussed in the previous section, lone pairs of two more O atoms (O5 and O7) in $Ca(TFSI)_2$ and $Ba(TFSI)_2$ are also involved in these interactions.

An interesting trend is found. The calculated order of main orbital interaction energies (E_{int}) parallels that of E_{bind}, although E_{int} only accounts for part of the E_{bind}. In fact, the E_{int} could be roughly attributed to the covalency contributions to binding. Thus, the covalency fraction of anion−cation interactions can be estimated as following order: LiTFSI (35%) > $Cu(TFSI)_2$ (26%), $Zn(TFSI)_2$ (27%), $Mg(TFSI)_2$ (28%) > $Ca(TFSI)_2$ (10%) > $Ba(TFSI)_2$ (5%). The main trend of this order is due to changes in the hard/soft mismatch between the cation and the anion. As the hardest and smallest one among alkaline earth metal cations, Mg^{2+} would approach and interact with oxygen atoms (hard base) at most ease leading to the largest covalency contribution in divalent metal−oxygen bond. The same trend was also obtained by Magnusson.[35] The lithium−oxygen bond still holds bigger covalency fraction than all of the divalent metal−oxygen bonds. As to copper and zinc ion complexes, small ionic radius ($r_{Cu^{2+}} = 0.72$ Å, $r_{Zn^{2+}} = 0.83$ Å) allows them to interact with O atoms easily, so both have considerable covalency fraction.

From the charge delocalizing point of view, we could conclude that large E_{int} means strong charge delocalization from O atoms to cations, as well as less positive charges on cations.

TABLE 4: NBO Energetic Analysis for Various Metal−TFSI⁻ Ion Pairs (Energies in kcal/mol)

vicinal interactions[a]	$Cu(TFSI)_2$	$Zn(TFSI)_2$	$Mg(TFSI)_2$	$Ca(TFSI)_2$	$Ba(TFSI)_2$	LiTFSI
$n^1_{O1} \rightarrow n^*_M$	7.03	12.61	19.87	4.57	2.25	7.97
$n^2_{O1} \rightarrow n^*_M$	0.12	0.09	14.89	1.77	0.53	
$n^3_{O1} \rightarrow n^*_M$	27.21	23.42	0.20	0.90	0.31	0.55
$n^1_{O2} \rightarrow n^*_M$	7.57	12.61	18.95	7.42	3.67	8.02
$n^2_{O2} \rightarrow n^*_M$	0.37	0.09	0.59	0.33	0.08	
$n^3_{O2} \rightarrow n^*_M$	32.63	23.42	16.48	0.16		0.57
$n^1_{O3} \rightarrow n^*_M$	7.58	12.61	18.98	4.51	2.22	
$n^2_{O3} \rightarrow n^*_M$	32.86	0.09	0.50	1.75	0.52	
$n^3_{O3} \rightarrow n^*_M$	0.39	23.42	16.24	0.93	0.27	
$n^1_{O4} \rightarrow n^*_M$	7.27	12.61	19.99	7.41	3.65	
$n^2_{O4} \rightarrow n^*_M$	0.14	0.09	14.56	0.31	0.07	
$n^3_{O4} \rightarrow n^*_M$	28.61	23.42	0.24	0.17		
$n^1_{O5} \rightarrow n^*_M$				4.18	2.16	
$n^2_{O5} \rightarrow n^*_M$				1.68	0.52	
$n^3_{O5} \rightarrow n^*_M$				0.88	0.31	
$n^1_{O7} \rightarrow n^*_M$				4.22	2.16	
$n^2_{O7} \rightarrow n^*_M$				1.69	0.51	
$n^3_{O7} \rightarrow n^*_M$				0.88	0.26	
$E_{orbital}$	151.78	144.44	141.49	43.83	19.52	17.11

[a] n^1_O, n^2_O, and n^3_O refer to the p lone pairs of the oxygen atoms; n^*_M refers to the antibonding orbital of lone pairs of the metal cations.

TABLE 5: Comparison of Catalytic Ability of Metal Complexes Lewis Acids in Diels−Alder Reaction[a]

	$Cu(TFSI)_2$	$Zn(TFSI)_2$	$Mg(TFSI)_2$	$Ca(TFSI)_2$	$Ba(TFSI)_2$ [b]	LiTFSI	$Zn(Tf)_2$	$ZnCl_2$
E_{LUMO} (eV)	−4.681	−4.747	−4.659	−4.596	−4.315	−4.068	−4.341	−3.060
	−3332	**−3392**	**−3.276**	**−3.199**		**−2.737**	**−3.128**	**−2.596**
E_{HOMO} (eV)	−5.566	−9.054	−9.162	−8.928	−8.769	−8.482	−9.684	−9.119
	−4.517	−8.226	8.365	−8.047		−7.722	−8.885	−6.736
ΔE (eV)[c]	2.560	2.494	2.591	2.645	2.926	3.173	2.900	4.181
	3.666	3.392	3.722	3.799		4.260	3.870	4.402
Z/r[d]	1.262	1.558	1.917	1.547	1.299	1.061	1.392	0.853
Z/r[e]	1.953	2.117	2.421	1.803	1.412	1.356	2.035	1.581
E_{bind}	578.6	536.8	509.3	417.9	359.9	48.4	536.8	604.1
	503.7	489.7	446.5	351.4		109.7	530.5	624.9
k_{obs} [f]	1370	125	18	5	1	1		23

[a] The bold value is obtained at B3LYP/6-31G* level. [b] The basis set for Ba is out of range of 6-31G*, so the calculation at B3LYP/6-31G* level cannot be performed for $Ba(TFSI)_2$. [c] E_{HOMO} of acrolein is −7.241 eV (B3LYP/lanl2dz) or −6.998 eV (B3LYP/6-31G*//B3LYP/lanl2dz). [d] The Mulliken effective cation charge. [e] The NPA effective cation charge. [f] Reference 6.

The Mulliken charges and NPA charges presented in Table 2 prove our conclusion. Furthermore, if we calculate the charge-transfer interaction E_{CT} by NPA population decrease of metal cations, the same trends as E_{bind} and E_{int} could also be obtained.

Catalysis. The motive driving us to initiate this investigation is to explore quantitatively the excellent Lewis acidity and catalytic ability of $M(TFSI)_2$ and to make some reasonable predictions according to the rules obtained through calculations. So in this section, we will discuss the theoretical results correlated with experimental data[5,6] about the catalysis of $M(TFSI)_2$ in Diels−Alder reaction of cyclopentadiene and methyl acrolein.

As generally recognized, the normal electron demand Diels−Alder reaction is a $LUMO_{dienophile}$−$HOMO_{diene}$-controlled reaction. The basic concept of activation in this reaction is to utilize the lone pair of the carbonyl group in the dienophile for coordination to the Lewis acid catalyst. It can also be described as the LUMO orbital of Lewis acid attacks the HOMO orbital of dienophile leading to a decrease in both HOMO and LUMO energy levels of the dienophile. So lower LUMO energy level of Lewis acid produces an easier and stronger attack on the HOMO orbital of dienophile, and thus greater decrease of FMO energies of dienophile, which leads to a better activation, as well as a lower energy barrier.

Calculated LUMO energy levels are listed in Table 5, together with ΔE (energy difference between $LUMO_{Lewisacid}$ and $HOMO_{dienophile}$) and effective cation charges. The observed rate constants are included for comparison.[6]

Generally, the orbital energies obtained at B3LYP/lanl2dz level give reasonable results with one deviation for $Cu(TFSI)_2$. An obvious rule can be found that lower LUMO energy levels of $M(TFSI)_x$ produce smaller ΔE's and larger rate constants. This is in very much accordance with the discussion above. Though relevant experimental data for the catalysis of $Zn(Tf)_2$ in this Diels−Alder reaction is not available at hand, reasonable predictions could also be made. Comparison among $Zn(TFSI)_2$, $Zn(Tf)_2$, and $ZnCl_2$ indicates that metal complex containing weaker coordinating anions usually holds larger effective cation charge and lower LUMO energy level, which results in a faster reaction.

The deviation of $Cu(TFSI)_2$ in the LUMO energy trend does not mean lower catalytic activity than $Zn(TFSI)_2$ because $Cu(TFSI)_2$ has a unique feature—its HOMO orbital only has a single electron. NBO analysis of $Cu(TFSI)_2$ revealed that the single-electron HOMO orbital is a $3d_{xy}$ valence orbital, which has a low occupancy of 1.350. So it is quite possible for this orbital to accept extra electrons and take part in the coordination with the carbonyl group in the dienophile. Further, the calculated HOMO energy of $Cu(TFSI)_2$ (−5.362 eV) is still higher than that of acrolein (−7.241 eV). So from the energy approximation point of view, this HOMO orbital should be able to interact with the HOMO orbital of acrolein. As to other $M(TFSI)_2$ species, their HOMO energies are much lower than that of acrolein suggesting no interactions between them. The extra HOMO−HOMO interaction between aceolein and $Cu(TFSI)_2$ might account for the outstanding catalytic activity of this copper

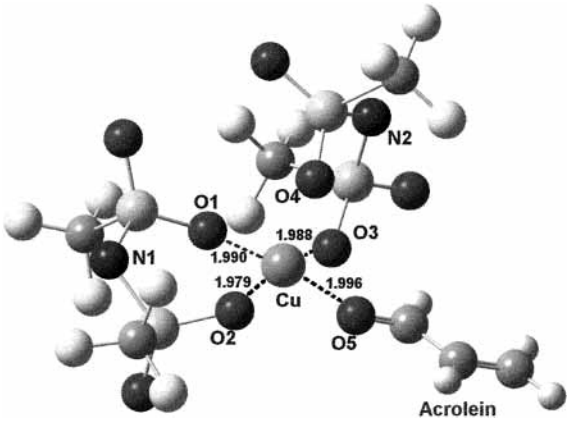

Figure 2. Optimized geometry of acrolein−Cu(TFSI)$_2$ complex.

salt. In addition, the planar square coordinating structure of Cu^{2+} in Cu(TFSI)$_2$ also facilitates the attack of acrolein from both sides of the O1−O2−O4−O3 plane.

For group 1 and group 2 metal bis(trimethylsulfonyl)imides, the increase in effective cation charge parallels the increase in rate constant. This is consistent with our previous report,[6] as well as the research of Casaschi et al. on catalysis of perchlorates in similar Diels−Alder reactions.[36] When one takes into account the transition metal complexes, the effective cation charge fails to interpret the experimental results indicating its limitation in comparing transition metal complexes with main group metal complexes.

E_{bind} is also listed in Table 5, because we note that the E_{bind} increases in parallel with the increase of rate constant. This suggests there might be some kind of relation between the binding energy and catalytic activity of these metal complexes. But a definite conclusion cannot be drawn until a thorough theoretical and experimental investigation on the catalysis of other metal complex series is carried out. Related research on metal triflates and metal chlorides has been carried out in our group, and similar trends are also found.[37] These comparisons are better made between species with same the cations or anions.

To further study the interactions between Lewis acids and dienophile, we used acrolein as a dienophile model to complex with the Lewis acids. After geometry optimization, we found that zinc and copper metal complexes still maintain quandradentate coordination with one metal−oxygen bond replaced by a metal−carbonyl bond while pentadentate structures are obtained for alkaline earth metal complexes. The optimized structure of acrolein−Cu(TFSI)$_2$ complex was given in Figure 2. The distance between the O4 atom and Cu atom is 2.169 Å, It's longer than the sum of ionic radii of oxygen and copper atoms (2.07 Å) suggesting no significant interaction between the two atoms. The O1−O2−O5−O3 dihedral angle is −4.75° showing that the Cu^{2+} still keeps a planar square coordinating structure. NBO calculation was performed because this deletion procedure permits us to study intramolecular delocalization interactions by coupling any two orbitals on separate fragments in the complexes. So it can afford a more detailed quantitative description on these interactions.

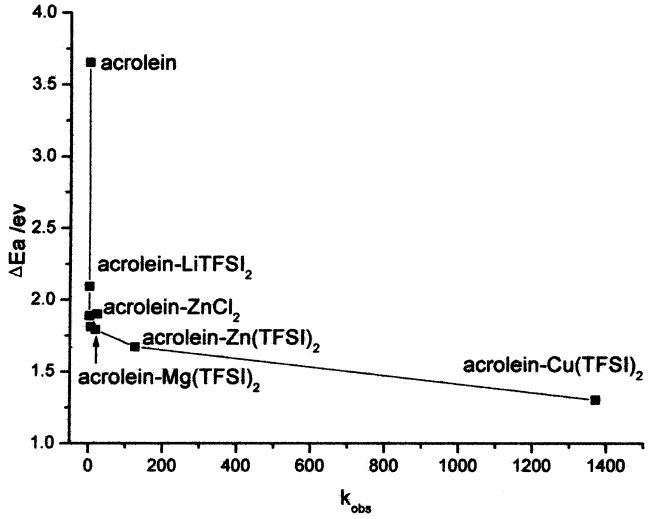

Figure 3. Relations between k_{obs} and ΔE_a. E_{HOMO} of cyclopentadiene is −5.947 eV (B3LYP/lanl2dz).

As Table 6 reveals, upon complexation with Lewis acids, the HOMO and LUMO energies of acrolein significantly decrease. The biggest LUMO decrease occurs for Cu(TFSI)$_2$−acrolein complex up to 2.350 eV (B3LYP/lanl2dz level). The activation barrier ΔE_a, which is roughly defined as the difference between $LUMO_{dienophile}$ and $HOMO_{diene}$, could be estimated. Figure 3 describes the relations between ΔE_a and k_{obs}. NBO analysis shows that the lone pairs of O atom (n^1_O and n^2_O) in acrolein interact most with the antibonding orbital (n*(6)M for copper and zinc complexes or n*(1)M for group 1 and group 2 complexes) of cations, which means strong charge delocalization from O to M^{2+}. Interestingly, the magnitude of the delocalization interaction energies reproduces the same trend as the LUMO energies.

However, discrepancy does exist between calculation results and experimental data for Mg(TFSI)$_2$, which shows larger E_{del} while smaller k_{obs} than $ZnCl_2$. It's probably because as a harder acid than zinc salts (see effective cation charges in Table 5) Mg(TFSI)$_2$ is more sensitive to the hard base H_2O and liable to be deactivated by the trace moisture in solvents or substrates. Nie's report[6] has already proved that the reaction catalyzed by dehydrated Mg(TFSI)$_2$ proceeds three times faster than that by hydrated catalyst Mg(TFSI)$_2$·3H_2O. As to the relatively softer zinc salts, the hydrated Zn(TFSI)$_2$·3H_2O demonstrated the same catalytic activity as dehydrated Zn(TFSI)$_2$.

Another point should be addressed that significant empty d orbital interaction is observed in acrolein−Cu(TFSI)$_2$ through NBO analysis. We found that all of the n*(6)M or n*(1)M orbitals in acrolein−metal−TFSI complexes are predominantly (>99%) s character, while in acrolein−Cu(TFSI)$_2$ complex, another antibonding orbital assigned as n*(5)Cu has a hybrid of p (0.04%) and d (99.96%) character. This clearly is a d orbital, and the interaction between it and acrolein accounts for 31% of the total E_{del}, while no similar interaction is observed in other complexes. This d orbital involvement proves our explanation in the previous section and may to some extent explain the outstanding catalytic activity of Cu(TFSI)$_2$.

TABLE 6: Energetics of Dienophile−Lewis Acid Complexes at B3LYP/lanl2dz Level

	acrolein	$ZnCl_2$−acrolein	Zn(Tf)$_2$−acrolein	Zn(TFSI)$_2$−acrolein	Cu(TFSI)$_2$−acrolein	Mg(TFSI)$_2$−acrolein	Ca(TFSI)$_2$−acrolein	Ba(TFSI)$_2$−acrolein	LiTFSI−acrolein
E_{LUMO}	−2.294	4.045	−4.203	−4.502	−4.644	4.153	−4.135	−4.057	−3.853
E_{HOMO}	−7.241	−7.571	−8.614	−8.427	−5.362	−8.524	−8.659	−8.535	−8.032
E_{del} kcal		26.61	29.69	33.59	47.94	31.52	7.96	3.74	14.82

From the discussion in this section, we can conclude that effective cation charge is useful to compare the Lewis acidity of main group metal complexes, while FMO energies are effective to predict the Lewis acidity, as well as catalytic activity, for both transition metal and main group metal complexes. Binding energy might also be a good alternative to evaluate the catalytic property of these Lewis acids.

Predictions. Presently, our group is dedicated on the synthesis of a novel Lewis acid with following structure:

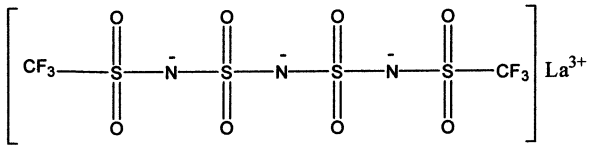

Having similar structure as $M(TFSI)_2$, this compound is expected to demonstrate special catalytic property owing to it's unique trivalent single-anion structure, which has three SO_2-N-SO_2 units. Herein, we would like to make a reasonable prediction on it's catalytic property through theoretical calculations at B3LYP/lanl2dz level and comparisons with $M(TFSI)_2$.

As expected, this compound has a fairly low LUMO energy level (−4.812 eV) comparable to that of $Zn(TFSI)_2$ (−4.747 eV). Its complex with acrolein also shows lower LUMO energy level (−4.646 eV) than $Cu(TFSI)_2$−acrolein (−4.644 eV). NBO analysis is not performed for the unparametrization of lanthanide atoms. Therefore, a strong Lewis acidity, as well as catalytic activity, could be predicted for this novel compound. It is a potential weakly coordinating species that could be used as an excellent Lewis acid catalyst. Experimental research is in progress.

Conclusions

We have presented a DFT study of the structures and cation−anion interactions of metal−TFSI complexes. Energetic calculations suggest that quandradentate structures are the most stable. NBO analyses indicate strong delocalization interactions involving the lone pairs of metal-chelated oxygen atoms and the antibonding orbitals of cations. Comparisons of binding energies and FMO energies among these metal complexes show that transition metal complexes hold stronger Lewis acidity than main group metal complexes. NBO analyses on the acrolein−Lewis acid complexes also reveal that because of the involvement of d orbitals, metal−TFSI complexes show higher catalytic activity. FMO energies are proved to be effective to evaluate the catalytic property of Lewis acid. And our calculations further proved that metal−TFSI complexes are better Lewis acid catalysts than metal triflates and metal chlorides.

Further theoretical research on scandium and lanthanide bis(trifluoromethylsulfonyl)imides is under the way.

Acknowledgment. We thank gratefully Guizhou High Performance Computation Center for its generous amount of calculation time. We thank the National Science Foundation of China (Grant No. 59873008) and Education Ministry of China (Grant No. 2234) for their supports.

References and Notes

(1) Bochmann, M. *Angew. Chem., Int. End. Engl.* **1992**, *31*, 1181.
(2) Seppelt, M. *Angew. Chem., Int. End. Engl.* **1993**, *32*, 1025.
(3) Strauss, S. H. *Chem. Rev.* **1993**, *93*, 927.
(4) Foropoulos, J.; DesMarteau, D. D. *Inorg Chem.* **1984**, *23*, 3720.
(5) Kobayashi, H.; Nie, J.; Sonoda, T. *Chem. Lett.* **1995**, 307.
(6) Nie, J.; Kobayashi, H.; Sonoda, T. *Catal. Today* **1997**, *36*, 81.
(7) Nie, J.; Xu, J.; Zhou, G.-Y. *J. Chem. Res.(S)* **1999**, 446.
(8) Ishihara, K.; Kubota, M.; Yamamoto, H. *Synlett* **1996**, 265.
(9) Mikami, K.; Kotera, O.; Motoyama, Y.; Sakaguchi, H.; Martuta, M. *Synlett* **1996**, 171.
(10) Armand, M.; Gauthier, M.; Muller, D. U.S. Patent No. 4,851,307, 1989.
(11) Vallee, A.; Besner, S.; Prud'homme, J. *Electrochim. Acta* **1992**, *37* (9), 1579.
(12) Dominey, L. A.; Koch, V. R.; Blakley, T. J. *Electrochim. Acta* **1992**, *37*, 1551.
(13) Benrabah, D.; Arnaud, R.; Sanchez, J.-Y. *Electrochim. Acta* **1995**, *40*, 2437.
(14) Arnaud, R.; Benrabah, D.; Sanchez, J.-Y. *J. Phys. Chem.* **1996**, *100*, 10882.
(15) Gejji, S. P.; Suresh, C. H.; Babu, K.; Cadre, S. R. *J. Phys. Chem. A* **1999**, *103*, 7474.
(16) Johansson, P.; Gejji, S. P.; Tegenfeldt, J.; Lindgren, J. *Electrochim. Acta* **1998**, *43*, 1375.
(17) Rey, I.; Johansson, P.; Lindgren, J.; Lassègues, J. C.; Grondin, J.; Servant, L. *J. Phys. Chem. A* **1998**, *102*, 3249.
(18) Hass, A.; Klare, Ch.; Betz, P.; Bruckmann, J.; Krüger, C.; Tsay, Y.-H.; Aubke, F. *Inorg. Chem.* **1996**, *35*, 1918.
(19) Zak, Z.; Ruzicka, A. *Z. Kristallogr.* **1998**, *213*, 217.
(20) Becke, A. D. *J. Chem. Phys.* **1993**, *98*, 5648.
(21) Lee, C.; Yang, W.; Parr, R. G. *Phys. Rev. B* **1988**, *37*, 785.
(22) Hay, P. J.; Wadt, W. R. *J. Chem. Phys.* **1985**, *82*, 270.
(23) Su, M.-D.; Chu, S.-Y. *J. Am. Chem. Soc.* **1997**, *119*, 5373.
(24) Legge, F. S.; Nyberg, G. L.; Peel, J. B. *J. Phys. Chem. A* **2001**, *105*, 7905.
(25) Stewart, J. J. P. *J. Comput. Chem.* **1989**, *10*, 209.
(26) Halgren, T. A. *J. Comput. Chem.* **1996**, *17*, 490 and following papers in this issue.
(27) Glendening, E. D.; Reed, A. E.; Carpenter, E.; Weinhold, F. *NBO*, version 3.1.
(28) *PC Spartan Prol.07*; Wavefunction, Inc.: Irvine, Califonia.
(29) Frisch, M. J.; Trucks, G. W.; Schlegel, H. B.; Scuseria, G. E.; Robb, M. A.; Cheeseman, J. R.; Zakrzewski, V. G.; Montgomery, J. A., Jr.; Stratmann, R. E.; Burant, J. C.; Dapprich, S.; Millam, J. M.; Daniels, A. D.; Kudin, K. N.; Strain, M. C.; Farkas, O.; Tomasi, J.; Barone, V.; Cossi, M.; Cammi, R.; Mennucci, B.; Pomelli, C.; Adamo, C.; Clifford, S.; Ochterski, J.; Petersson, G. A.; Ayala, P. Y.; Cui, Q.; Morokuma, K.; Malick, D. K.; Rabuck, A. D.; Raghavachari, K.; Foresman, J. B.; Cioslowski, J.; Ortiz, J. V.; Stefanov, B. B.; Liu, G.; Liashenko, A.; Piskorz, P.; Komaromi, I.; Gomperts, R.; Martin, R. L.; Fox, D. J.; Keith, T.; Al-Laham, M. A.; Peng, C. Y.; Nanayakkara, A.; Gonzalez, C.; Challacombe, M.; Gill, P. M. W.; Johnson, B. G.; Chen, W.; Wong, M. W.; Andres, J. L.; Head-Gordon, M.; Replogle, E. S.; Pople, J. A. *Gaussian 98*; Gaussian, Inc.: Pittsburgh, PA, 1998.
(30) Zhang, X.-Y.; et al. *Applied Chemistry Handbook*; Beijing Chemical Industry Press: 1986; Chapter 1.
(31) Bakker, A.; Gejji, S.; Lindgren J.; Hermansson, K.; Probst, M. M. *Polymer* **1995**, *36*, 4371.
(32) Reed, A. E.; Curtiss, L. A.; Weinhold, F. *Chem. Rev.* **1988**, *88*, 899.
(33) Rulišek, L.; Havlas, Z. *J. Am. Chem. Soc.* **2000**, *122*, 10428.
(34) Rulišek, L.; Havlas, Z. *J. Phys. Chem. A* **2002**, *106*, 3855.
(35) Magnusson, E. *J. Phys. Chem.* **1994**, *98*, 12558.
(36) Casaschi, A.; Desmoni, G.; Faita, G.; Invernizzi, A. G.; Lanati, S.; Righetti, P. P. *J. Am. Chem. Soc.* **1993**, *115*, 8002.
(37) Li, X.-Y.; Nie, J., manuscript in preparation.